Journal of Applied Electrochemistry (2006) 36:1297–1306
DOI 10.1007/s10800-006-9187-y

Towards a determination of the active surface area of polycrystalline and nanoparticle electrodes by Cu upd and CO oxidation

T. NAGEL, N. BOGOLOWSKI and H. BALTRUSCHAT*
Institut für Physikalische Chemie, Universität Bonn, Römerstrasse 164, D 53117, Bonn, Germany
*(*author for correspondence, tel.: + 49-228-73-4162; fax: + 49-228-73-4160; e-mail: baltruschat@uni-bonn.de)*

Received 17 October 2005; accepted in revised form 30 May 2006

Key words: Cu-UPD, CO-oxidation, DEMS, Pt-single crystal electrodes, Se-deposition, surface area determination, Ru-electrode

Abstract

Methods for the determination of the surface area for Pt, Ru and Se modified Pt and Ru are compared, in view of their possible application for technical and nanoparticle electrodes. The hydrogen adsorption charge can hardly be used as a reliable measure for the surface area for Ru because it is paralleled by anion adsorption. The charge necessary for the oxidation of adsorbed CO also contains a large contribution due to anion or oxygen adsorption, which amounts to approx. 45% of the charge in the case of Ru. The mass spectrometrically determined amount of CO_2 formed gives a more reliable measure for the surface area, provided that the maximum coverages are constant and independent of the particular surface. Values obtained in this way agree to within 20% with surface area values obtained from measuring the charge needed for the desorption of a complete monolayer of Cu upd on Pt(111) and polycrystalline Pt, polycrystalline Ru, submonolayers of Ru on polycrystalline Pt and on Pt(111) and for nanoparticle, carbon supported electrodes. Se modified Ru has recently found attention as a methanol tolerant cathode material for oxygen reduction. CO does not adsorb on Pt or Ru saturated by Se. For surfaces partially covered by Se, a comparison of the charge measured by cyclic voltammetry in the hydrogen region and of the mass spectrometrically determined amount of CO_2 suggests that the latter can be used for a determination of the area not covered by Se. Cu upd, on the other hand, also takes place on surfaces completely covered by Se; the Cu desorption charge is independent of the Se coverage on Pt and Ru modified Pt as long as it does not exceed 70% of full coverage. In the presence of multilayers of Se, Cu_xSe is formed. On Se modified bulk Ru the amount of Cu upd decreases with increasing Se coverage, approaching only 105 μC m^{-2} for full Se coverage.

1. Introduction

One of the main reasons for the low efficiency of PEM fuel cells is the high overvoltage of the oxygen reduction reaction (ORR). In the case of the direct methanol fuel cell (DMFC) this overvoltage is increased due to methanol crossover from the anode to the cathode, which may be poisoned by methanol. To avoid this problem, Tributsch et al. [1–3] suggested use of a $RuSe_x$ catalyst, which is completely unreactive towards methanol, but shows good reactivity towards oxygen reduction. In order to compare the reactivity of different catalysts it would be advantageous to relate the activity to the real surface area of the different catalysts [4].

In the case of a pure Pt-catalyst the real surface area is usually determined from the hydrogen adsorption charge. For Pt/Ru, the charge for the oxidation of adsorbed CO may be used as a measure for the surface area. A problem, however, arises due to the fact that even after the usual background subtraction, approximately 45% of the oxidation charge on Pt/Ru catalysts is merely a pseudo capacitive charge, whereas on pure Pt this pseudo capacitive effect amounts to 20% [5]. This charge is due to the fact, that in the double-layer region anions (or oxide species) are adsorbed on Pt, which are displaced when CO is adsorbed and then are readsorbed upon oxidation of CO. It is directly measurable in charge displacement experiments with CO [6–8].

Differential electrochemical mass spectrometry (DEMS) is able to differentiate between the CO oxidation currents and capacitive effects and will therefore be used here. Whereas CO adsorbs on both Ru and Pt it does not adsorb on Se [9]. An alternative method therefore is necessary. Kucernak and coworkers showed that upd of Cu occurs at different potentials on Ru and Pt; therefore they were able to determine the relative surface concentrations of Ru and Pt [10]. The main aim of this paper is to elucidate whether the surface area of Se modified Ru catalysts can be determined via Cu upd. Se modified Pt electrodes will be examined for comparison.

2. Experimental

Measurements were done in an electrochemical H-cell in the hanging meniscus arrangement and with DEMS using a thin layer cell. The dual thin layer flow through cell used in the present study was described in detail elsewhere [5, 11, 12]. This cell was used for DEMS in combination with a quadrupole mass spectrometer (Pfeiffer Vacuum QMG 422). It consists of two separate compartments: the electrochemical compartment with the electrolyte inlet, where the faradaic reactions take place and the mass spectrometric compartment with the electrolyte outlet. Volatile species produced in the first compartment are transported through six capillaries to the second compartment, where they can evaporate into the mass spectrometer and can be measured as ion current. The electrolyte volume and the nominal geometric surface area (0.28 cm^2) of the working electrode are defined by a thin (50–100 μm) PTFE ring on the disc shaped working electrode. The reference electrode was a reversible hydrogen electrode (RHE). Two Pt wires were used as counter electrodes. The experiments were performed at room temperature, with a potential sweep rate of 10 mV s^{-1} (unless otherwise noted). The upper limit of the potential scans was set to 900 mV for all Ru containing catalysts in order to avoid dissolution of Ru.

As the working electrodes we used disc shaped single crystals with a diameter of 1 cm with the orientations Pt(111) from Metal Crystals & Oxides, UK, a smooth polycrystalline Pt electrode, or carbon supported Pt nanoparticles attached to glassy carbon (GC). Prior to each experiment single crystals were prepared by flame annealing according to the method of Clavilier [13]: the crystals were heated to red colour in a hydrogen or propane flame and cooled for 4 min in ultra pure Argon. Glassy carbon disc electrodes with a diameter of 10 mm, polished to a mirror finish, were used as a substrate for the carbon supported catalysts [14]. The colloidal platinum particles (40% wt. Pt), supported on Vulcan XC 72 were obtained from E-TEK, Inc (Lot # C0510517). Ru colloids (20% wt. Ru) were prepared by the group of Prof. Bönnemann from Karlsruhe [15, 16]. For the electrode preparation, a definite volume (in the range of 20 to 30 μl) of an ultrasonically dispersed catalyst in ethylene glycol was pipetted onto the glassy carbon substrate, creating a catalyst film with platinum or ruthenium loading of 10 μg_{metal} cm^{-2} (suspensions in ethylene glycol resulted in smoother deposits than suspensions in water). After evaporating the solvent (at 80–100 °C), the deposited Pt catalysts were covered with 82 μl of Nafion solution in water at a concentration of ca. 1.44 mg ml^{-1} and dried at ambient temperature. The aqueous solution of Nafion was prepared by diluting the commercial solution in isopropanol (Aldrich) with water and subsequent evaporation of the isopropanol. The resulting Nafion film with a thickness of about 1 μm was of sufficient strength to permanently attach the catalyst particles to the glassy carbon electrode [14]. All solutions were prepared using ultrapure water (Millipore; 18.2 MΩ m, < 3 ppb TOC) and ultrapure analytical grade or suprapure chemicals from Merck and Fluka, and deaerated by high purity (99.999%) Ar; and CO of 99.997% purity from Praxair was used for preparing CO saturated solutions.

Different Ru or Ru modified polycrystalline Pt and Pt(111) electrodes were prepared from a 5×10^{-3} M $RuCl_3$ solution according to Geyzers [17, 18].

Multilayers of Ru on Pt were deposited at 50 mV (deposition time 10 min) resulting in a roughness factor $R_f \approx 1.2$. The roughness factor was determined by relating the CO oxidation charge on the geometric area of the electrode surface. (Sub-) monolayers of Ru on Pt were adsorbed at different constant potentials between 300 and 700 mV with a deposition time of 5 min.

Se was deposited by adsorbing a full monolayer at open circuit or by gradual deposition under potential control. Procedure A, the gradual deposition of Se in the thin layer flow through cell used for DEMS involved potential-cycling between 50 and 300 mV for several potential cycles in 5×10^{-7} M H_2SeO_3 in 0.5 M H_2SO_4. Procedure B, used in an H-cell without forced convection, was similar to A, but the concentration was 5×10^{-6} M H_2SeO_3 in 0.5 M H_2SO_4, and the potential range 50–800 mV.

In procedure C, the deposition of a full monolayer by adsorption from 10^{-5} M H_2SeO_3 and 0.5 M H_2SO_4 at open circuit potential was followed by partial dissolution of Se in a potential scan up to 1100 mV [19].

CO was adsorbed at a constant electrode potential of 70 mV by replacing the 0.5 M H_2SO_4 solution with a 0.5 M H_2SO_4 solution saturated with CO (ca. 10^{-3} M). After the formation of a CO monolayer, the solution was exchanged by pure 0.5 M H_2SO_4 solution under potential control (E = 70 mV), in order to have a solution free of CO. Then the adsorbed CO was oxidized to CO_2 during the positive potential sweep. The CO oxidation on polycrystalline Pt is done for comparison and also serves for the determination of the calibration constant K^* of the experimental setup [12, 20]. K^* is the ratio between the integrated ionic current (Q_i) of the mass spectrometer and the faradaic current (Q_f) when the current efficiency is 100%, taking into account the number of electrons (z = 2 for the oxidation of CO) and that 20% of the charge obtained by integration of the background corrected current is still due to double layer charging. The currents were integrated between 350 and 900 mV, except for Pt(111) when the integration limits were 500 and 900 mV.

$$K^* = zQ_i/Q_f \tag{1}$$

The true surface area of Se free catalysts was calculated from the ionic charge for m/z = 44 according to:

$$A^i_{t,CO} = \frac{Q_f}{K^* F \Gamma_M} \tag{2a}$$

where F is faraday constant and Γ_m is surface concentration of a monolayer of CO.

For comparison it was also calculated from the faradaic oxidation charge:

$$A^{f}_{t,CO} = \frac{Q_f}{zF\Gamma_m} \quad (2b)$$

where z is number of electrons

We assume a maximum CO coverage (CO molecules per Pt sites) of 1.45 nmol cm^{-2}, corresponding to 280 μC cm^{-2}. This is an average value often observed on different smooth and stepped Pt surfaces [8, 21, 22]. The same Γ_m was assumed to hold for the Ru modified surfaces.

The relative Se coverage was determined via co-adsorption of CO. Since CO does not adsorb on Pt [9] or Ru (see below) fully covered by Se, the CO oxidation charge on surfaces partially covered by Se corresponds to the free Pt or Ru sites. Therefore, with $\Theta_{Se} + \Theta_{CO} = 1$,

$$\Theta^{CO}_{Se} = 1 - \frac{Q^{CO}_{MSe}}{Q^{CO}_{M}} = \frac{Q^{CO}_{M} - Q^{CO}_{MSe}}{Q^{CO}_{M}} \quad (3a)$$

Here, Q^{CO} is the true faradaic CO oxidation charge without double-layer contributions as calculated from the ionic charge and M represents Pt or Ru.

This procedure for the calculation of surfaces not totally covered by Se is more reliable than using the suppression of hydrogen adsorption. On Ru the hydrogen adsorption is largely paralleled by anion and oxygen adsorption. Especially for colloid-electrodes a "hydrogen adsorption" potential range is not well defined.

Nevertheless, for comparison, in addition to Θ^{CO}_{Se}, the coverage with Se was determined by the charge of hydrogen adsorption in the range of 50–350 mV, without any subtraction for double-layer charge.

$$\Theta^{H} = \frac{Q^{H}_{MSe}}{Q^{H}_{M}} \quad (3b)$$

Cu upd was performed in 10^{-3} M $CuSO_4$ in 0.5 M H_2SO_4 solution during a potential sweep down to 50 mV, followed by a potential stop at 300 mV during the anodic sweep for different times (60–180 s). In preliminary measurements (not shown here) the charges for Cu upd were not well reproducible and clearly lower than expected for a monolayer. We assume that Cu deposition (and adsorption) on Ru is inhibited during the cathodic sweep due to the readsorbed OH. Therefore, we used the more complicated procedure where the Ru surface is first reduced at lower potentials. Excess bulk Cu deposited at this low potential is dissolved during the potential stop at 300 mV. Desorption of upd Cu is achieved by sweeping up to 900 mV [10], in some case only up to 700 mV. The charge for the Cu upd desorption peak was determined by integration from 300 to 700 mV after background subtraction of the corresponding charge in the copper free sulfuric acid. From Cu upd the surface area is calculated as mentioned by Kucernak [10]:

$$A_{t,Cu} = \frac{Q^{f}_{Cuupd}}{420\ \mu C\ cm^{-2}} \quad (4)$$

3. Results and discussion

3.1. *Selenium deposition*

On a Ru-modified Pt-surface two possible sites for selenium adsorption exist. When modifying the bimetallic Pt/Ru surface with Se, a primary question is whether Se interacts preferably with Pt or with Ru. On Ru modified Pt(111), a distinction is possible because of the very specific structure sensitive sulfate adsorption peak. On Pt(111) Ru is known to adsorb in islands which have a typical width of 2–3 nm [18, 23–26]. Upon increasing the Ru coverage only their number, not the size, increases. At least at low Ru coverages, in between these islands the space is large enough for the formation of the ordered sulfate adlayer; the typical spike at 450 mV is therefore visible (cf. Figure 1A). Consequently, if Se adsorbs preferentially on top of the Ru islands, in an experiment where Se is allowed to adsorb slowly from a dilute solution, the charge of the sulfate adsorption peak should not decrease immediately and initially more slowly than that of the charge in the hydrogen region. However, if Se adsorbs on Pt first, the sulphate adsorption should decrease rapidly due to its structure sensitivity (sulfate adsorption is known to be strong only on large Pt(111) domains with a diameter above 1–2 nm). The sulfate adsorption involves long range order effects and is thus over-proportional to the number of free Pt(111) sites. It can therefore also be expected to decrease over-proportionally when the number of sites decreases due to adsorption of Se. Therefore, from the relation between the suppression of the hydrogen-adsorption and the sulfate-adsorption it should be possible to decide where Se adsorbs on the Pt(111)/Ru-surface.

The voltammogramms of Ru-modified Pt(111) are shown in Figure 1A and those during the Se adsorption on Pt(111)/Ru are shown in Figure 1B and C. At the beginning, the hydrogen-region is hardly suppressed. With increasing time of potential-cycling in Se-containing solution both the currents in the hydrogen and sulfate region decrease. The dependence of the charge Q^{H} in the hydrogen region on the charge Q^{SO_4} in the sulfate region is shown in Figure 1D for different Ru-coverages. As can be seen from Figure 1D for low Ru-coverages Q^{SO_4} decreases at a slower rate than Q^{H}. Since this is also true for the Pt(111) without Ru, this indicates the formation of domains of Se and/or a repulsive

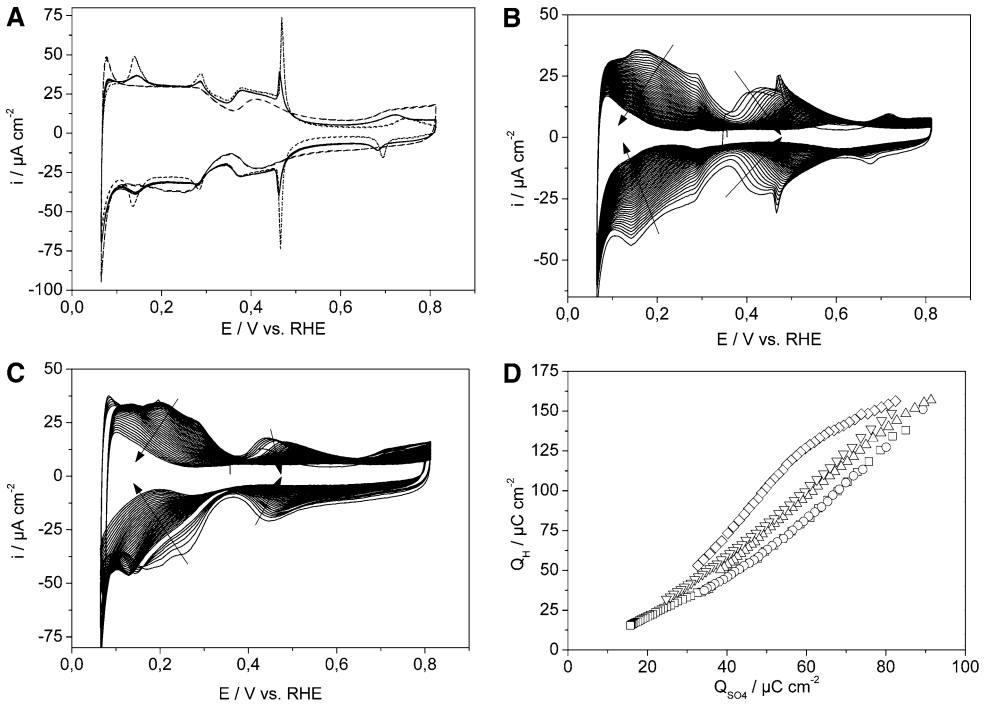

Fig. 1. Effect of Se deposition on the CV of Pt(111) and Pt(111) modified by Ru (scan rate 50 mV s^{-1}, H-cell). (A) CV of Pt(111) covered with different Ru submonolayers in 0.5 M H_2SO_4: clean Pt(111) ($\Theta_{Ru} = 0$, dotted line), Pt(111)/Ru ($\Theta_{Ru} = 0.2$, straight line) and Pt(111)/Ru ($\Theta_{Ru} = 0.35$, dashed line). (B) CVs of Pt(111)/Ru ($\Theta_{Ru} = 0.2$) in 5×10^{-6} M H_2SeO_3 in 0.5 M H_2SO_4. (C) CVs of Pt(111)/Ru ($\Theta_{Ru} = 0.35$) in 5×10^{-6} M H_2SeO_3 in 0.5 M H_2SO_4. (D) Plot of Q^H vs. Q^{SO_4} with increasing number of cycles (increasing Se coverage) on Pt(111)/Ru with different Ru coverage (cf. (B) or (C)), $\square\Theta_{Ru} = 0$ (only Se), $\bigcirc\Theta_{Ru}$ = very low (adsorption of Ru for 2 min at open circuit) $\triangle\Theta_{Ru} = 0.2$ ($E_{ad} = 700$ mV), $\triangledown\Theta_{Ru} = 0.25$ ($E_{ad} = 600$ mV), $\diamond\Theta_{Ru} = 0.35$ ($E_{ad} = 500|$mV). Se adsorption was done by procedure B.

interaction of Se with adsorbed hydrogen. At higher Ru-coverages Q^{SO_4} shows a faster decrease than Q^H. Thus we can assume that Se does not adsorb preferentially on Ru.

Figure 2 shows the effect of increasing coverage of Se on the CV of multilayers of Ru deposited on polycrystalline Pt electrodes. With increasing Se coverage, the hydrogen adsorption and anion desorption is decreased and the CV loses its characteristic features. This is in agreement with the suppression of the hydrogen adsorption charge on pure Pt [9].

3.2. *Anodic stripping of CO*

The voltammogramms of the oxidative desorption of co-adsorbed CO on Pt or Pt/Ru electrodes modified with Se submonolayers are shown in Figure 3. The amount of Se was varied by adsorbing a full monolayer of Se, followed by partial dissolution of Se (procedure C) for each stripping experiment.

At the polycrystalline Pt-substrate the CO oxidation peak is shifted from 700 to 800 mV with increasing Se coverage. At high Se coverage the CO adsorption is totally suppressed [9]. On the Se modified Pt(111) the oxidation peak for CO remains around 800 mV, independent on the Se coverage. For Pt(pc) modified with Ru and Se (Figure 3B) there is only a decrease in the amount of adsorbed and oxidized CO detectable. The strongly negative potential shift of the CO oxidation peak (Figure 3D) to 400 mV due to Ru adsorbed on Pt(111), and in particular the shoulder at 500 mV arising from CO adsorbed at some distance of Ru, has already been previously reported [25, 26]. For the system Pt(111)/Ru/Se the CO oxidation peak is again shifted to more positive potentials due to Se. Se obviously overcompensates the catalytic effect of Ru.

On Pt-surfaces, the suppression of the hydrogen-adsorption charge is usually taken as a measure for the

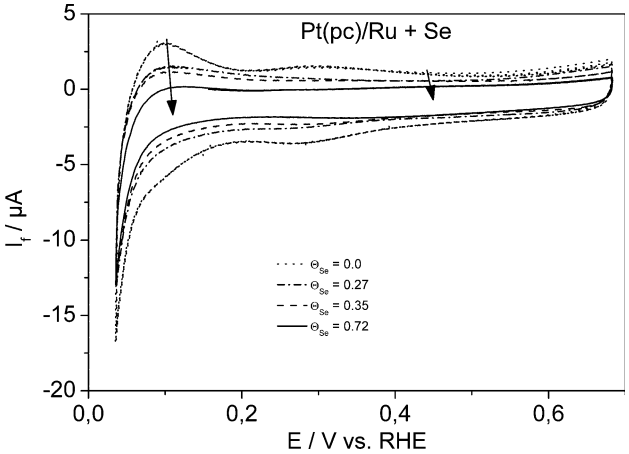

Fig. 2. CVs of Ru deposited in multilayers on Pt(pc) and partially covered by Se in 0.5 M H_2SO_4: $\Theta_{Se} = 0.0$ (dotted line), $\Theta_{Se} = 0.27$ and $\Theta_{Se} = 0.35$ (both dashed lines), and $\Theta_{Se} = 0.72$ (straight line). Se deposition by procedure A in the DEMS flow-through cell. Arrows indicate increasing Se coverage. Scan-rate 10 mV s^{-1}, Roughness factor 1.2.

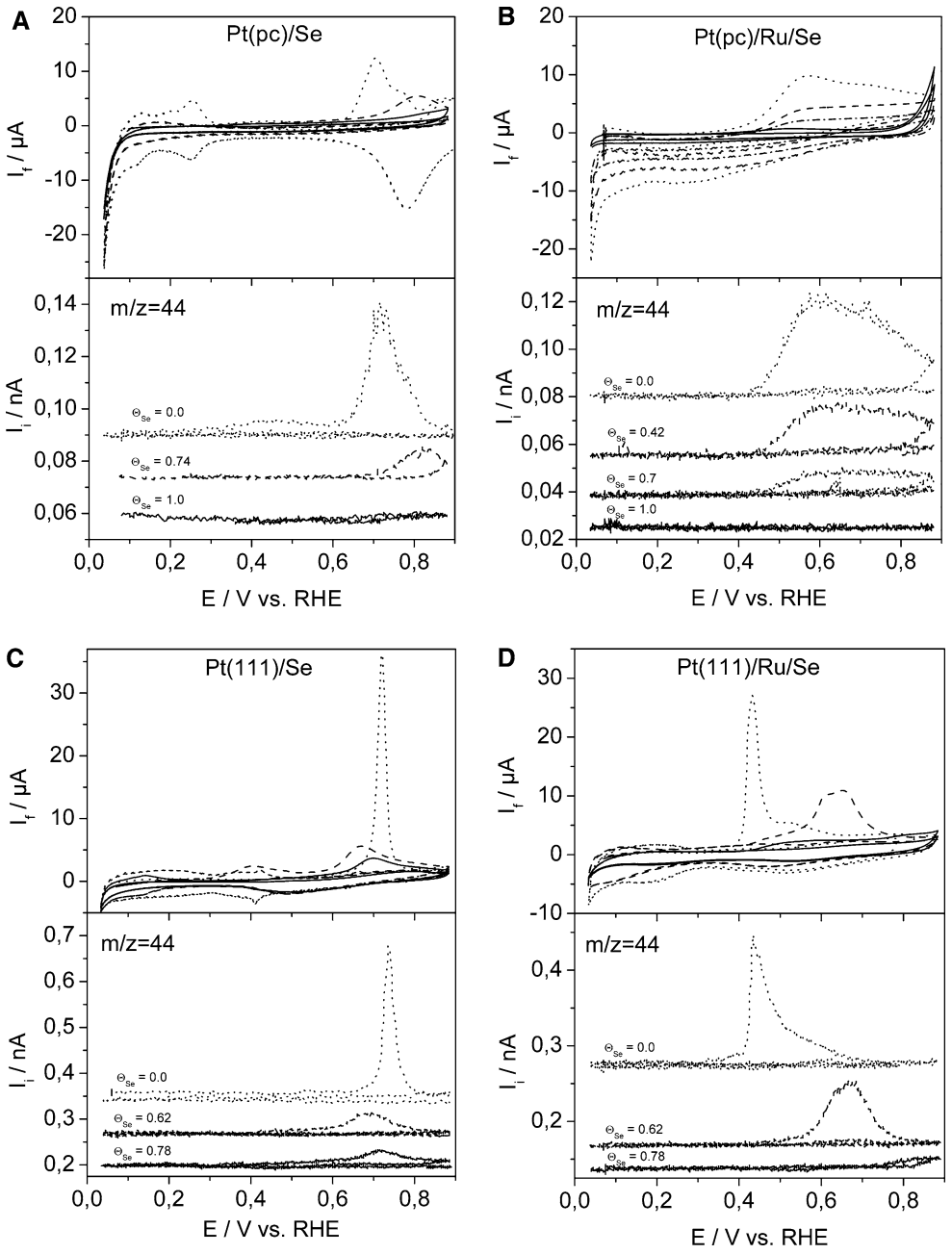

Fig. 3. Simultaneously recorded CVs and MSCVs (m/z = 44) in the DEMS-cell for the oxidation of adsorbed CO on different electrodes pre-covered with Se. (A) Pt(pc) with Θ_{Se} = 0 (dotted line), 0.74 (dashed line) and 1 (straight line). (B) Ru deposited in multilayers on Pt(pc) and modified by different amounts of Se: Θ_{Se} = 0 (dotted line), 0.42 (dashed line), 0.70 (dash-dotted line) and 1 (straight line). (C) Pt(111) with Θ_{Se} = 0 (dotted line), 0.62 (dashed line), 0.78 (straight line). (D) Pt(111)/Ru ($\Theta_{Ru} \approx 0.3$) with Θ_{Se} = 0 (dotted line), 0.26 (dashed line) and 0.88 (straight line). Deposition of Se was done by procedure C. Baselines in MSCVs shifted for better visibility. Scan-rate 10 mV s^{-1}.

coverage with another species, like Se in our case. Therefore, in Figure 4 the hydrogen coverage Θ^H, calculated from the adsorption charge for hydrogen (Equation 3B), is plotted vs. the selenium coverage as determined from the CO adsorption experiments. For comparison, despite the limited reliability of the charge assignment to hydrogen-adsorption in the case of Ru, we include the corresponding results for Pt/Ru in the graph.

The inset in Figure 4 shows the increase in Se coverage with number of cycles during the deposition via procedure A reaching complete coverage of the substrate with Se after 40 cycles for Pt(pc) surfaces covered by Ru mono- or multilayers.

For Pt(111) and polycrystalline Pt the hydrogen coverage correlates linearly with the Se coverage as determined from CO coadsorption, in agreement with [9] for Pt(111). The intercept of the linear fit with the x-axis is at $\Theta^{CO}{}_{Se} = 1$.

3.3. *Copper upd*

Desorption of upd Cu from Pt(111) gives rise to only one desorption peak around 700 mV (Figure 5). lts peak

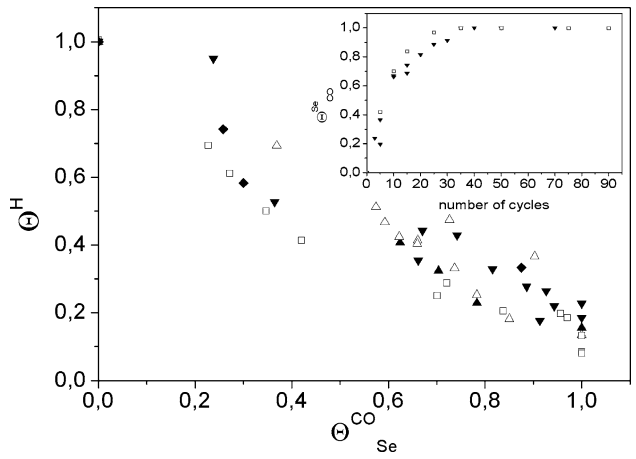

Fig. 4. Plot of the suppression of hydrogen coverage vs. the CO coverage calculated from the corresponding CVs/MSCVs (cf. Figure 3): □ Pt(pc)/Ru(multilayers)/Se (procedure A), ▼ Pt(pc)/Ru($\Theta_{Ru} \approx 0.25$)/Se (procedure A), △ Pt(pc)/Se (procedure C), ▲ Pt(111)/Se (procedure C), ◆ Pt(111)/Ru($\Theta_{Ru} \approx 0.3$)/Se (procedure C). Inset: Increase of the Se coverage with the numbers of cycles (procedure A); Θ^{CO}_{Se} was calculated from the suppression of CO adsorption using the corresponding MSCV data; symbols as above.

position its very much dependent on sweep rate (at 10 mV s^{-1} the peak is centered at 650 mV), and at sweep rates below 0.1 mV s^{-1}, a peak splitting is sometimes observed [29–33]. On Ru covered Pt(111), the peak for Cu at Pt sites shifts to lower potentials; the shift of the deposition peaks to higher potentials in the cathodic sweep indicates a higher reversibility, which is probably caused by the disorder induced by Ru islands. With increasing Ru coverage, a new peak for Cu desorbing from Ru sites emerges around 400 mV.

Since anions (hydroxide or oxide) adsorb much stronger at Ru than at Pt, it is not apriori clear to what degree a contribution of adsorbing anions is included in this peak. For the Cu upd peak at Pt(111) the amount of anions adsorbed at the Cu monolayer is similar to that at Pt(111) and thus the experimentally determined charge of 420 μC cm^{-2} is close to the theoretical value of 480 μC cm^{-2} for a $2e^-$ process. This charge was used to calculate the Pt area on the surfaces partially covered by Ru and the Ru coverage was then calculated according to:

$$\Theta_{Ru} = 1 - \frac{Q^{Pt}_{Cu\,upd}}{420\,\mu C\ cm^{-2}} \qquad (5)$$

The dependence of the Ru coverage on the potential of Ru deposition is depicted in the inset of Figure 5, and agrees well with that previously determined by XPS [18].

Figure 6 shows the CVs of bare and Se modified Pt electrodes in Cu-containing sulfuric acid. The Cu upd desorption peaks on polycrystalline Pt (at 550, 600 and 700 mV) and on Pt(111) (at 650 mV) in Figure 6A and C have been described in [10, 33]. The different peaks or shoulders at the CV of polycrystalline Pt are due to the different single crystal facets. The peak for the Cu upd dissolution appears at 350 mV for Se on platinum as described in [34]. The peak for removal of Cu on the Ru electrode (Figure 6B) has been discussed by Green et al. [10]. For the multilayer Ru electrode there is no additional peak visible at potentials higher than 700 mV which would correspond to a pure Pt surface (Figure 6A). For a mixed Pt/Ru surface one would expect an additional peak at 750 mV. Therefore, this surface is completely covered by Ru. For the Se modified Pt(pc) surface, the Cu upd desorption peak appears at 350–400 mV, as observed before on pure Pt. The peak for the removal of Cu upd strongly increases for high coverages of Se. At $\Theta_{Se} = 1$ a new peak evolves at about 400 mV. In the case of Se deposition on Pt(111) for Cu upd removal three new peaks appear (Figure 6C). The peaks at 420 and 380 mV are visible at lower Se coverage; at a Se coverage above $\Theta_{Se} = 0.78$ the peak at 320 mV appears. These peaks are also observed on the polycrystalline Pt, but less clearly. Riveros et al. [35] deposited Cu onto multilayers of Se on a gold substrate; dissolution of Cu from the Cu_xSe phase also gave rise to 2 peaks at 330 and 210 mV vs. SCE.

In Figure 6D there are two peaks visible for the Cu upd desorption, corresponding to the desorption of copper from Ru (350 mV) and Pt (550 mV) [10]. If the dissolution of Se predominately occurred from Ru, the Cu upd peak corresponding to Pt would decrease at low Se coverages (Figure 6D). This tendency cannot be clearly seen and implies that there is no preferential adsorption of Se either on Ru or Pt, as stated before for Pt(111) (cf. Figure 1) where Se was gradually deposited.

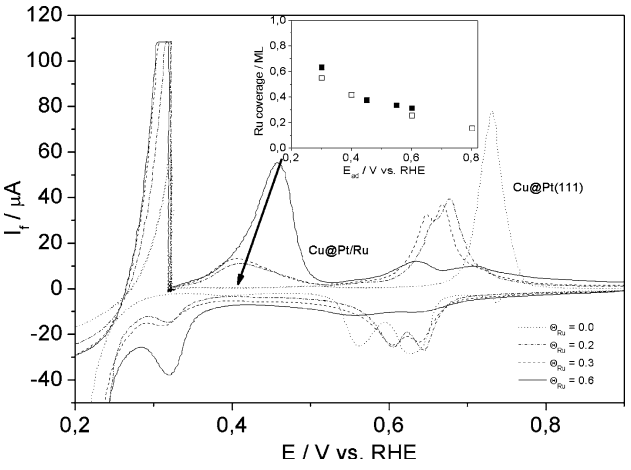

Fig. 5. CVs of Cu upd on Pt(111) covered with different Ru submonolayers in 10^{-3} M $CuSO_4$ + 0.5 M H_2SO_4: bare Pt(111) ($\Theta_{Ru} = 0$, dotted line) and Pt(111)/Ru ($\Theta_{Ru} = 0.2$, dash-dotted line; $\Theta_{Ru} = 0.3$, dashed line; $\Theta_{Ru} = 0.6$, straight line). Arrow indicates decreasing Ru coverage. Scan-rate 10 mV s^{-1}; H-cell. Dissolution of bulk Cu at 300 mV for 60 s. Inset: Plot of Ru-coverage vs. adsorption-potential for 5 min Ru adsorption from 5×10^{-3} M $RuCl_3$ solution in 0.5 M H_2SO_4 on Pt(111). Ru-coverage determined from charge of Cu upd dissolution (closed symbols, see text for details) and from XPS (open symbols, results taken from [18]).

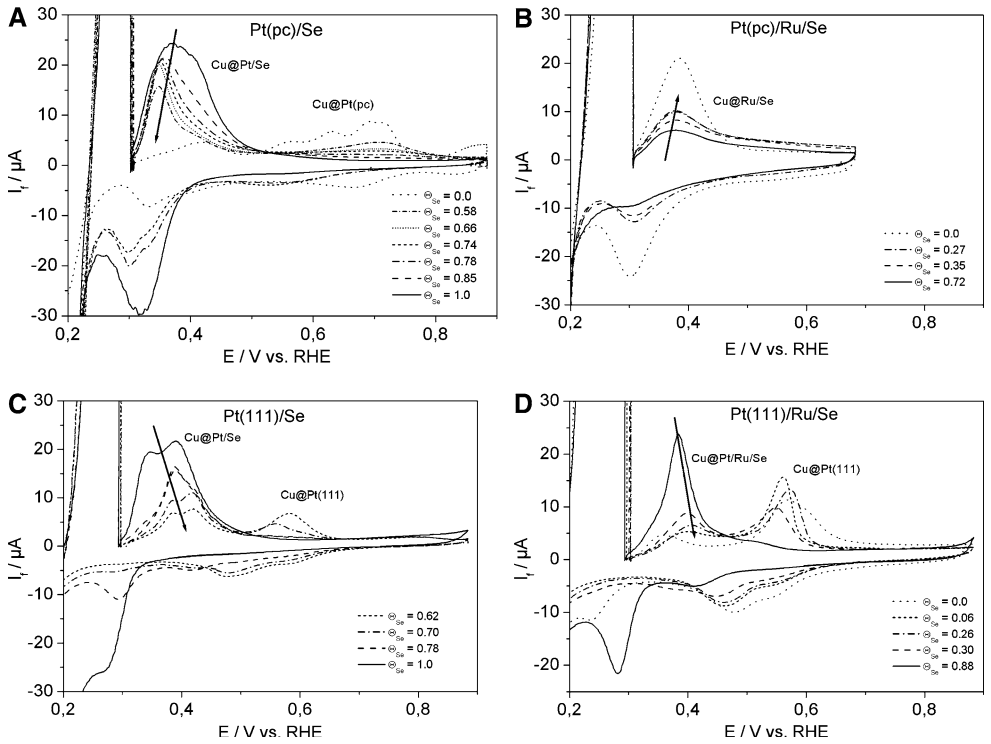

Fig. 6. CVs of Cu upd in 10^{-3} M $CuSO_4$ + 0.5 M H_2SO_4 before Se deposition (dotted line) and with different Se coverage (as indicated in the figure, the highest Se content is depicted by a straight line) (A) Pt(pc). (B) Pt(pc)/Ru multilayers. (C) Pt(111). (D) Pt(111)/Ru($\Theta_{Ru}\approx0.3$). Deposition of Se was done by procedure C. Arrows indicate decreasing Se coverage. Scan-rate 10 mV s^{-1}; DEMS-cell. Dissolution of bulk Cu at 300 mV for 60 s.

3.4. *Surface area calculations for pure Ru electrodes*

Table 1 summarizes the charges for Cu upd desorption and CO_{ad} oxidation from Figure 3 and 6. The areas are calculated according to Equations 2 and 4.

The differences in the areas calculated from the mass spectrometric ion current and the faradaic ion current during CO oxidation reflect the pseudo capacitive charges mentioned in the introduction section which, in the case of polycrystalline Pt, is 20% of the CO oxidation current. For Pt(111) 26% of the CO oxidation charge corresponds to pseudo capacitive effects, which is equivalent to the charge of sulfate adsorption of about 90 μC cm^{-2} on Pt(111) [21, 22]. This high contribution is due to the fact that the lower integration limit, including that of the background subtraction, is positive of the sulfate adsorption peak.

In the case of Ru, even after background subtraction, the faradaic charge for the CO oxidation on Ru or Ru modified surfaces is, taking the average, 80% higher than the oxidation charge for the CO as calculated from the amount of CO_2 formed ($Q_{CO\ mass\ spectrometric}$). In other words, 45% of the oxidation charge is due to non-faradaic processes, in accordance with [5]. We have to assume that after stripping of CO_{ad} and returning to the starting potential (E = 350 mV) in the double layer region, the surface is recovered by OH and the overall process has to be described by:

Table 1 Comparison of the charges and corresponding surface areas by the different methods. Cu upd charge (data from Figure 6), CO stripping charge obtained from the amount of CO_2 (data from Figure 3) and CO stripping charge from CV (data from Figure 3, charge with double-layer correction). Geometric surface area of the electrode is 0.28 cm^2

Substrate	Q_f/mC			A_t/cm^2			CO mass spectrometric/ CO faradaic
	Cu upd	CO mass spectrometric	CO faradaic	Cu upd	CO mass spectrometric	CO faradaic	
Pt(pc)	0.185	0.134	0.172	0.44	0.48	0.61	0.78
Pt-colloid	0.635	0.468	0.602	1.51	1.67	2.15	0.78
Pt(111)	0.111	0.079	0.107	0.26	0.28	0.38	0.74
Pt(111)/Ru($\Theta_{Ru} \approx 0.3$)	0.142	0.095	0.165	0.34	0.34	0.59	0.58
Pt(pc)/Ru($\Theta_{Ru} \approx 0.6$)	0.116	0.086	0.187	0.28	0.31	0.67	0.46
Pt(pc)/Ru($\Theta_{Ru} \approx 0.25$)	0.125	0.094	0.163	0.30	0.34	0.58	0.58
Pt(pc)/Ru	0.189	0.101	0.196	0.45	0.36	0.70	0.52
Ru-colloid	0.845	0.830	1.342	2.01	2.97	4.80	0.62

$$\mathrm{RuCO} + (1+x)\mathrm{H_2O} \rightarrow 2\mathrm{e}^- + \mathrm{CO_2} + \mathrm{Ru(OH)}_x + x\mathrm{e}^- + x\mathrm{H}^+ \quad (6)$$

More exactly, since the coverage of Ru by CO is approximately 0.7, we expect the number of electrons per Ru surface atom is 1.4 for the oxidation of CO. As mentioned above, the experimental value for the faradaic charge is 80% higher, i.e. 2.5 electrons per Ru atom. The difference of one electron corresponds to the adsorption of OH; therefore $x \approx 1$ in Equation 6.

The area calculated from the Cu desorption charge agrees to within 20% with the area calculated from the amount of CO_2 detected during CO oxidation (except for Ru-colloid). Non-faradaic contributions to the Cu desorption charge are therefore small. Since, as shown above, Ru is covered by anionic species at the lower integration limit of 300 mV, the conclusion can be drawn that, on the Cu surface, nearly the same amount of anions were adsorbed as on the bare Ru surface.

The agreement of the area determined from Cu upd and CO stripping suggests that the assumption of a maximum CO coverage of 70% also holds for the nanoparticles. This is in disagreement with [36, 37], where the CO oxidation charge was compared to the hydrogen adsorption charge and a ratio of 2:1 was obtained. As discussed already [38], this result is not caused by a CO coverage of 1 on the nanoparticles, but more likely by a diminished hydrogen adsorption. We cannot exclude the possibility that the Cu coverage is also increased with respect to that at a polycrystalline electrode. For a 2-nm particle, between 10 and 20% Cu atoms might be adsorbed at edge sites in addition to the full coverage corresponding to a Pt:Cu ratio of 100%. However, these should not be strongly bound, and desorb at potentials close to the bulk Cu dissolution; they are probably not included in our integration. The area of the Ru nanoparticles as determined from Cu upd seems to be too small because at the lower integration limit of 300 mV Cu coverage at Ru nanoparticles may be less than 100%.

3.5. *Dependence of the Cu upd process on Se coverage*

The charge of Se coverage as determined from suppression of CO adsorption (Equation 3) and of the Cu upd charge during Se adsorption according to procedure A is plotted in Figure 7. The Se coverages increase clearly with the number of cycles and after 30–40 cycles a monolayer of Se on the Pt/Ru is established. The dependence of the coverage with Se on the number of cycles was discussed in the previous section. The increase in the charge for Cu upd begins with $\Theta > 0.8$ in the case of a Ru monolayer. The continuing growth of the Se coverage correlates linearly with the increase of Cu upd charge. If copper deposition was only possible on the top Se layer, there would only be one monolayer of Cu during the upd process (rejecting

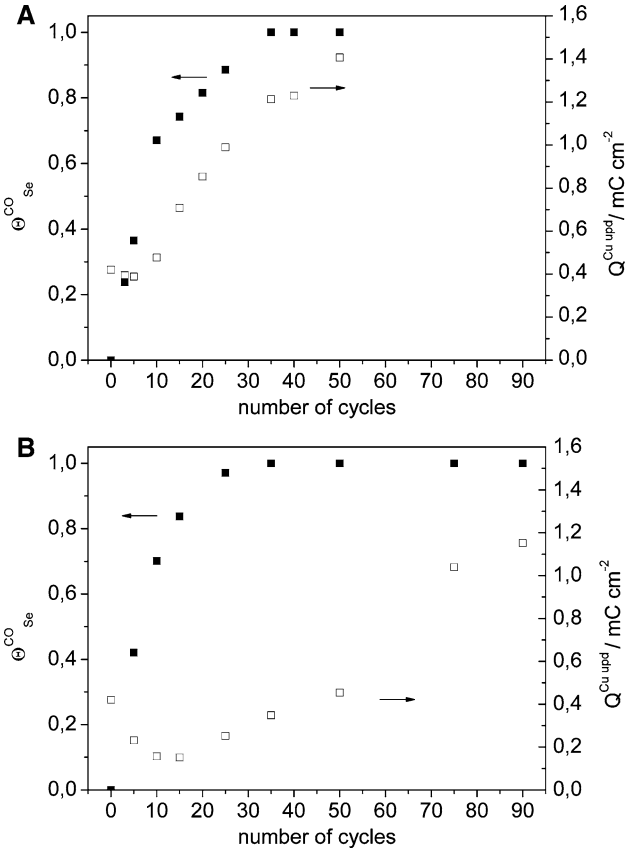

Fig. 7. Se coverage (determined from CO coadsorption) and charge of Cu upd as function of the number of Se deposition cycle. Deposition of Se was done by procedure A. ■ $\Theta^{CO}{}_{Se}$ calculated from the suppression of CO adsorption; □ charge of Cu upd dissolution. (A) monolayer of Ru on Pt(pc). (B) multilayer of Ru on Pt(pc).

the effect due to change in the surface roughness by Se multilayer adsorption), and the Cu charge would not increase further. The further increase in Cu charge therefore implies that Cu_xSe is formed [39].

Figure 8 shows the dependence of Cu upd charge on the Se coverage for different electrode surfaces. The charge for Cu upd is normalized to the surface determined by Cu upd on the Se free surface.

$$Q^{\mathrm{Cu\ upd}} = \frac{Q^{\mathrm{Cu\ upd}}_{\mathrm{exp}}}{A_{\mathrm{t,Cu}}} = \frac{Q^{\mathrm{Cu\ upd}}_{\mathrm{exp}}}{Q^{\mathrm{Cu\ upd}}_{0}} \cdot 420\,\mu\mathrm{C\ cm}^{-2} \quad (7)$$

In the case of pure Pt or a Ru monolayer (Figure 8A) the charge for the removal of Cu upd does not vary with Se coverage up to $\Theta_{Se} = 0.6$. Steponavicius et al. showed that the Cu upd removal charges for polycrystalline Pt and Pt with $\Theta_{Se} = 0.3$ are identical [34]. For Se coverages higher than 0.6, and in particular multilayers (which are not distinguishable from $\Theta_{Se} = 1$ using the CO adsorption method) the Cu charge increases due to the formation of Cu_xSe. Referring to the Pourbaix diagram, the formation Cu_2Se with $pH < 1$ is possible at potentials between -600 and 500 mV vs. NHE, at potentials up to 700 mV Cu_1Se is stable[39]. The increase in the Cu upd charge at $\Theta_{Se} < 1$

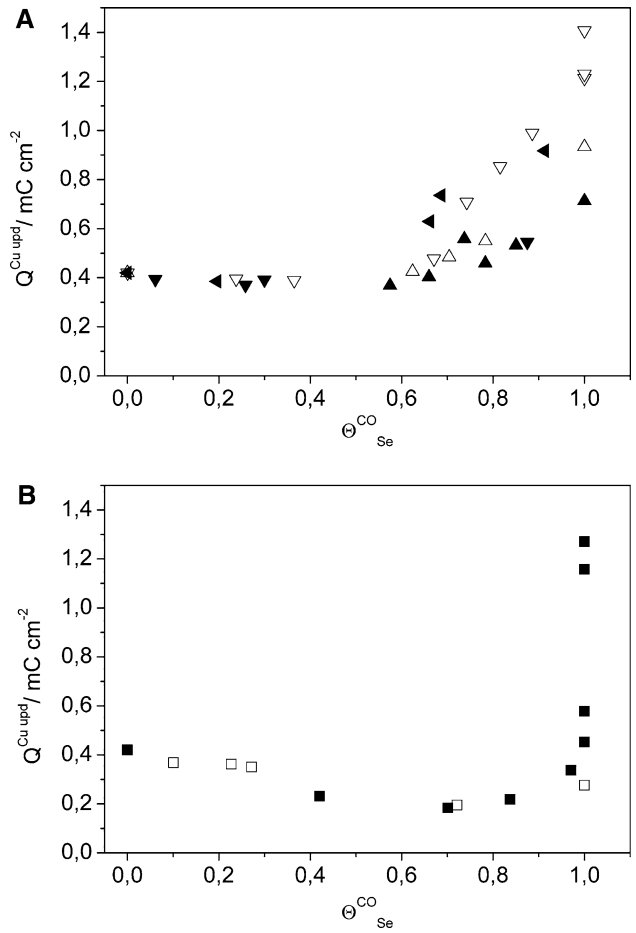

Fig. 8 Charge of Cu upd dissolution vs. $\Theta^{CO}{}_{Se}$ calculated from the suppression of CO adsorption. (A) no Ru or Ru monolayer only: ▲ Pt(pc)/Se (procedure C), △ Pt(111)/Se (procedure C), ▼ Pt(111)/Ru($\Theta_{Ru} \approx 0.3$)/Se (procedure C), ◀ Pt(pc)/Ru($\Theta_{Ru} \approx 0.25$)/Se (procedure C) and ▽ Pt(pc)/Ru($\Theta_{Ru} \approx 1$)/Se (procedure A). (B) Ru multilayer on Pt(pc): □ Pt(pc)/Ru/Se (procedure C), ■ Pt/Ru/Se (procedure A).

may in part be explained by the presence of steps: the "last" Se atom of a monolayer deposited at the edge can be seen as the beginning of the second layer. Another interpretation could be that Se is deposited on Ru in 3D-islands, which are able to grow into the second layer before the surface is close-packed. Furthermore, Cu might also attract Se from the monolayer to form a 3D Cu_xSe compound. Unfortunately, there is no potential at which only a monolayer of Se is stable at any surface in the accessible potential window: The Nernst equilibrium potential for Se/H_2Se0_3 is 740 mV [40], a potential at which Ru is oxidized. Dissolution of bulk Se as H_2Se is thermodynamically only possible below -300 mV.

A further possible problem must be considered. CO might compress the Se adlayer, and this would lead to coverage values according to Equation 3a which are too low [19].

In the case of massive Ru-electrodes (multilayers), the increase in Cu charge starts at $\Theta_{Se} = 0.9$. The value of the Cu upd charge extrapolated to a full monolayer of selenium is 105 μC cm^{-2} (Figure 8B). This is only a fourth of the Cu upd charge on the pure Ru electrode. In contrast to Figure 8A the substrate is bulk Ru, with other properties than just a monolayer of Ru on a Pt substrate. Probably, a $RuSe_x$ compound is formed only at the Ru multilayer surface, onto which only smaller amounts of Cu can adsorb and no Cu_xSe can be formed. This result is valid for Ru/Se surfaces both prepared by gradual deposition of Se (procedure A) and by partial dissolution of Se after deposition at open circuit (procedure C).

A reason for the lower charge could be the incomplete dissolution of Cu upd from the surface. It might be argued that a certain amount of adsorbed copper is not oxidized in the anodic scan and is still present on the surface, maybe bound to Se. To check whether this was the case, we performed a control experiment where, after doing a Cu upd experiment on Pt(pc) with a monolayer of Se, we dissolved the copper, made a control CV in the Cu free sulfuric acid and repeated the Cu upd experiment in copper containing electrolyte. The charge found for dissolution of copper was the same in both Cu upd experiments. Riveros et al. also stated that the Cu is totally dissolved from the Cu_xSe phase on multilayers of Se on a gold substrate [35]. This implies that on multilayers of Ru-modified with Se no residual copper is on the electrode after the anodic stripping of Cu. We cannot exclude the possibility that, on bulk Ru covered by Se, no Cu can adsorbed at all. The minimum value measured around $\Theta_{Se} = 0.7$ would then be due to the formation of Cu_xSe at this coverage, as already discussed for Figure 8A. However, the initial decrease in the Cu charge below a coverage of 0.4 makes this interpretation unlikely.

3.6. *Conclusions*

The dependence of the Cu upd charge on Se surface coverage prohibits the straightforward determination of the surface area by Cu upd for a surface of unknown Se surface composition. However, together with a determination of the Se coverage by CO, a determination of the area should be possible. Alternatively, the catalyst might be saturated by Se and then the minimum value for Q^{Cu} for a $RuSe_x$ surface might be used for calculating the area. For surfaces partially covered with different unknown amounts of Ru and Se it is possible to determine the total surface area by Cu upd. The fraction of Se covered surface can be determined via CO stripping experiments. Further measurements, especially on the $RuSe_x$ colloids, will be performed.

Acknowledgements

Thanks are due to Prof. Dr. Helmut Bönnemann and K. S. Nagabhushana from Forschungszentrum Karlsruhe GmbH for the preparation of the ruthenium colloids. We acknowledge financial support to the BMBF within the framework of the O2rednet project.

References

1. H. Tributsch, M. Bron, M. Hilgendorff, H. Schulenburg, I. Dorbandt, V. Eyert, P. Bogdanoff and S. Fiechter, *J. Appl. Electrochem.* **31** (2001) 739.
2. M. Bron, P. Bogdanoff, S. Fiechter, M. Hilgendorff, J. Radnik, I. Dorbandt, H. Schulenburg and H. Tributsch, *J. Electroanal. Chem.* **517** (2001) 85.
3. M. Bron, P. Bogdanoff, S. Fiechter, I. Dorbandt, M. Hilgendorff, H. Schulenburg and H. Tributsch, *J. Electroanal. Chem.* **500** (2001) 510.
4. M. Neergat, D. Leveratto and U. Stimming, *Fuel Cells – From Fundamentals Syst* **2** (2002) 25.
5. Z. Jusys, H. Massong and H. Baltruschat, *J. Electrochem. Soc.* **146** (1999) 1093.
6. O. Wolter and J. Heitbaum, *Ber Bunsenges Phys. Chem.* **88** (1984) 6.
7. J. Willsau and J. Heitbaum, *Electrochim. Acta* **31** (1986) 943.
8. V. Climent, R. Gómez and M. Feliu, *Electrochim. Acta* **45** (1999) 629.
9. E. Herrero, A. Rodes, M. Pérez J, J.M. Feliu and A. Aldaz, *J. Electroanal. Chem.* **412** (1996) 165.
10. C.L. Green and A. Kucernak, *J. Phys. Chem. B* **106** (2002) 1036.
11. H. Wang, T. Löffler and H. Baltruschat, *J. Appl. Electrochem.* **31** (2001) 759.
12. H. Baltruschat, *J. Am. Soc. Mass Spectrom.* **15** (2004) 1693.
13. J. Clavilier, R. Faure, G. Guinet and R. Durand, *J. Electroanal. Chem.* **107** (1980) 205.
14. T.J. Schmidt, H.A. Gasteiger, G.D. Stab, P.M. Urban, D.M. Kolb and R.J. Behm, *J. Electrochem. Soc.* **145** (1998) 2354.
15. H. Bönnemann and K.S. Nagabhushana, *J. New Mat. Electrochem. Syst.* **7** (2004) 93.
16. V.I. Zaikovskii, K.S. Nagabhushana, V.V. Kriventsov, K.N. Loponov, S.V. Cherepanova, R.I. Kvon, H. Bonnemann, D.I. Kochubey and E.R. Savinova, *J. Phys. Chem. B* **110** (2006) 6881.
17. K.-P. Geyzers, Ph.D. Thesis; Universität Bonn, 1997.
18. S. Cramm, K.A. Friedrich, K.P. Geyzers, U. Stimming and R. Vogel, *Fresenius J. Anal. Chem.* **358** (1997) 189.
19. J.M. Feliu, R. Gomez, M.J. Llorca and A. Aldaz, *Surf. Sci.* **289** (1993) 152.
20. H. Baltruschat. *in* A. Wieckowski (ed.), Interfacial Electrochemistry, (Marcel Dekker, Inc., New York, Basel, 1999), pp. 577.
21. T. Hartung, U. Schmiemann, I. Kamphausen and H. Baltruschat, *Anal. Chem.* **63** (1991) 44.
22. Schmiemann U., Ph.D. Thesis; Universität Witten-Herdecke (1993).
23. K.A. Friedrich, K.P. Geyzers, A.J. Dickinson and U. Stimming, *J. Electroanal. Chem.* **524** (2002) 261.
24. K.A. Friedrich, K.-P. Geyzers, F. Henglein, A. Marmann, U. Stimming, W. Unkauf and R. Vogel (1996) *in* A. Wieckowski and K. Itaya (eds) 'Sixth International Symposium on Electrode Processes', Vol. 96-8 (The Electrochemical Society, Los Angeles), pp. 119–135.
25. D. Aberdam, F. Razafimaharo, R. Faure, R. Durand (1996) *in* A. Wieckowski, K. Itaya (eds), 'Sixth International Symposium on Electrode Processes', Vols. 96-8 (The Electrochemical Society, Los Angeles) pp. 280–286.
26. A. Crown, I.R. Moraes and A. Wieckowski, *J. Electroanal. Chem.* **500** (2001) 333.
27. H. Massong, H.S. Wang, G. Samjeske and H. Baltruschat, *Electrochim. Acta* **46** (2000) 701.
28. G. Samjeské, X.-Y. Xiao and H. Baltruschat, *Langmuir* **18** (2002) 4659.
29. A. Al-Akl and G.A. Attard, *J. Phys. Chem. B* **101** (1997) 4597.
30. C. Nishihara and H. Nozoye, *J. Electroanal. Chem.* **386** (1995) 75.
31. Y. Shingaya, H. Matsumoto, H. Ogasawara and M. Ito, *Surf. Sci.* **335** (1995) 23.
32. T. Abe, G.M. Swain, K. Sashikata and K. Itaya, *J. Electroanal. Chem.* **382** (1995) 73.
33. E. Herrero, L.J. Buller and H.D. Abruña, *Chem. Rev.* **101** (2001) 1897.
34. A. Steponavicius and D. Simkunaite, *Russ. J. Electrochem.* **38** (2002) 488.
35. G. Riveros, R. Henriquez, R. Cordova, R. Schrebler, E.A. Dalchiele and H. Gomez, *J. Electroanal. Chem.* **504** (2001) 160.
36. K.A. Friedrich, F. Henglein, U. Stimming and W. Unkauf, *Electrochim. Acta* **45** (2000) 3283.
37. F. Maillard, M. Eikerling, O.V. Cherstiouk, S. Schreier, E. Savinova and U. Stimming, *Faraday Discuss.* **125** (2004) 357.
38. B. Lanova, H. Wang, H. Baltruschat, *Fuel Cells*, **3–4** (2006)214.
39. P. Carbonnelle and L. Lamberts, *J. Electroanal. Chem.* **340** (1992) 53.
40. D. Lide, 'CRC Handbook of Chemistry and Physics' 80th edn., (CRC Press, Boca Raton, 1999).